International Journal on Magnetic Particle Imaging
Vol 8, No 1, Suppl 1, Article ID 2203001, 3 Pages

Infinite Science Publishing

Proceedings Article

Lissajous trajectory magnetic particle imaging for image-guided hyperthermia therapy and monitoring

J. Wells[a,*] · O. Kosch[a] · S. Twamley[b] · A. Ludwig[b] · J. Paeye[a,c] · H. Paysen[a] · F. Wiekhorst[a]

[a] Physikalisch-Technische Bundesanstalt, Berlin, Germany
[b] Medizinische Klinik für Kardiologie und Angiologie, Charité-Universitätsmedizin Berlin, Corporate Member of Freie Universität Berlin, Humboldt-Universität zu Berlin, and Berlin Institute of Health, Berlin, Germany
[c] Department of Solid State Sciences, Ghent University, Ghent, Belgium
*Corresponding author, email: james.wells@ptb.de

Abstract

Magnetic field hyperthermia (MFH) therapy is an emerging cancer treatment which uses heat to damage tumors. Like magnetic particle imaging (MPI), MFH combines injected magnetic nanoparticles with the subsequent application of time-varying magnetic fields. One potential application of MPI technology is in aiding the optimization and safety of MFH therapy. This work reports recent successes in demonstrating how Lissajous scanning magnetic particle imaging can act as a multi-functional platform to support the safe and optimized application of MFH therapy. Lissajous scanning MPI can i) image magnetic nanoparticles in-vivo to verify that they are correctly located within the tumor tissue before heat generation begins, ii) generate spatially-focused heating using the Lissajous scanning magnetic field sequences iii) produce 3D images of the elevated temperatures generated during therapy in real-time. Recent achievements in developing the capability for realizing accurately calibrated temperature-resolved 3D "multi-colour" Lissajous MPI via the system matrix technique are also reported.

I. Introduction

Magnetic field hyperthermia (MFH) is an emerging cancer therapy based on the localized heating of tumor tissue. The heat is generated by magnetic nanoparticles (MNPs) which are injected into the tumor site. High-frequency magnetic fields are then applied, causing the nanoparticles to dissipate heat into the immediately surrounding tissue. Nanoparticles accumulated within the tumor tissue create locally elevated temperatures damage or kill cancer cells, leaving the surrounding healthy tissues intact. MFH has received much interest and been the subject of several successful clinical trials. Multiple technical challenges remain to be solved before MFH therapy can reach regulatory approval and widespread use. These include improving the reliability and optimization of aspects such as the MNP heating efficiency, administration routes and heating dosimetry [2].

The potential of magnetic particle imaging (MPI) to support the realization of safe and optimized MFH has recently begun to be explored [3]. In this work, the capability of a Lissajous scanning MPI scanner to act as a multifunctional platform to support the successful administration of MFH therapy is explored.

10.18416/ijmpi.2022.2203001

II. Material and methods

The following subsections detail the apparatus and techniques implemented during the reported work.

II.I. MPI Scanner and Magnetic Nanoparticles

A Lissajous scanning MPI scanner (20/25 FF, Bruker Biospin, Germany) was used for all MPI measurements. Image reconstruction is based on a system function recorded using a point-like reference sample of known MNP content that is measured at defined points within the field of view.

The scanner is equipped with a bespoke additional gradiometric receive-only coil in one axis [4]. The commercial MNP system Ferucarbotran (FCT) (Meito Sangyo, Japan) was used in all experiments as a joint MPI tracer and MFH heating agent.

II.II. Characterizing hyperthermia during MPI

Spatially varying MFH induced during MPI image acquisitions was measured using small samples of FCT with varying concentration located at different points within the scanner's field of view. So far as possible, hyperthermia characterisation was done in line with the recommendations determined in [5]. Heating curves for MNP samples were measured using a fibre optic thermometer. To characterize the heat dissipation of a given combination of sample type, location and applied fields, the specific loss power (SLP) was calculated for each measured heating curve based on the corrected slope technique:

$$SLP = \frac{\left(C\frac{dT}{dt} + L\Delta T\right)}{m_{mnp}}$$

where C = specific heat capacity, ΔT = elevation of sample temperature above ambient at the point in heating curve used for SLP calculation, dT/dt = gradient of heating curve at that point in the heating curve, L = linear loss parameter specific to the particular sample and apparatus combination.

Maps of experimentally determined spatially varying SLP within the scanner were compared with simulations based on a phenomenological hyperthermia heat dissipation model developed for the project [6].

II.III. Tumour phantom measurements

Tumour phantoms were prepared using mixtures of THP-1 human acute monocytic leukemia cells mixed with FCT. The ability of the MPI scanner to image the location and concentration of the MNP inside the phantom, to heat the phantom via MFH, and to image the phantom temperature in real-time was then evaluated. After MFH exposure, the impact on the THP-1 cell population viability was measured by MTT ((3-(4,5-dimethylthiazol-2-yl)-2,5-diphenyl tetrazolium bromide) colorimetric assay of cellular metabolic activity. The impact on the cell membrane integrity was investigated by a 4',6-diamidino-2-phenylindol (DAPI) exclusion assay using flow cytometry.Control phantoms prepared using the same cell-MNP mix, but not exposed to MFH treatment were used to verify that the MFH treatment was the source of observed changes. Hyperthermia exposed phantoms were maintained at a base temperature of 37°C within the MPI scanner using a water-heated custom-built sample holder [6]. Figure 1 shows a photograph of a tumour phantom contained within an Eppendorf tube mounted within this heated sample holder. The pipes containing the heated water run under the insulation block containing the phantom. The fibre-optic thermometer is also labelled. Control phantoms were also maintained at 37°C throughout the period of the MPI exposure.

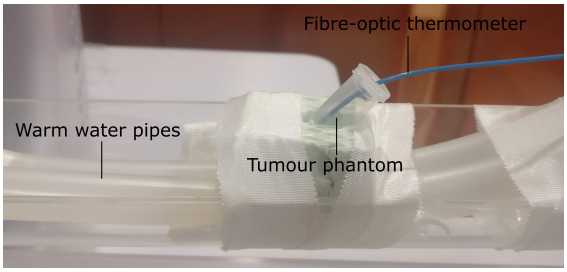

Figure 1: Photograph of a tumour phantom mounted on the temperature-regulated sample holder in preparation for magnetic field exposure within the MPI scanner.

II.IV. System Functions at Set Temperatures

An apparatus was built to enable control of the temperature of the MNP sample used during the recording of system functions for MPI reconstruction. System functions recorded at different temperatures can be used in the reconstruction of calibrated thermally resolved MPI images for remote thermometry [7]. The custom-built device employs a heated air stream to control the sample temperature and was demonstrated to show high accuracy and excellent stability (with $\Delta T < 0.1$ K).

III. Results and discussion

The spatial distribution of MFH heating generated by the magnetic field sequences of the Lissajous scanning MPI scanner was successfully mapped [6]. The results were compared with those produced by the phenomenologi-

10.18416/ijmpi.2022.2203001

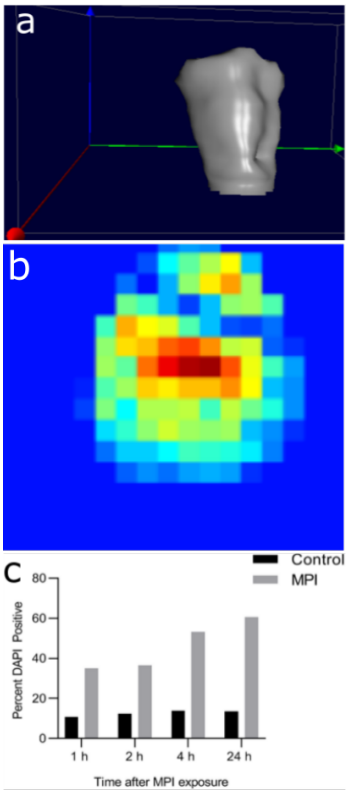

Figure 2: (a) MPI image of tumor phantom. (b) Temperature resolved MPI image during MFH treatment. (c) DAPI stained flow cytometry results during 24 hours following an 80 minute MFH exposure.

cal heating model. A good level of agreement was found between the model and the experimental observations.

The ability of Lissajous scanning MPI to act as a multifunctional platform for the provision of optimised and safe MPI was then explored. A summary of the key achievements are shown in figure 2. The capability of the MPI scanner to accurately image the distribution of magnetic nanoparticles within tumour phantoms was first demonstrated using short MPI exposures which generated no heating within the phantom (Fig. 2 (a)). Next, much longer (80 minute) MPI exposures were used to generate spatially localised heating within the tumour phantoms, while simultaneously monitoring the MPI signal produced by the sample during heating. After 80 minutes of exposure, maximum temperatures of 44.5°C were recorded. The ability of the MPI scanner to reconstruct thermally resolved images was demonstrated first with an uncalibrated technique (Fig 2. (b)) [6], and later using a calibrated technique based on "multicolour" MPI image reconstruction using system functions recorded using the equipment described in section II.IV.

Analysis of the tumour phantom cell populations 24 hours after the MFH exposure in the MPI scanner showed large numbers of damaged or dying cells as compared with the control samples. DAPI exclusion assay by flow cytometry showed that around 60 % of the treated cells have developed a leaky cell membrane after 24 hours (Fig 2 (c)). Similarly, MTT assays indicated significant inhibition of metabolic activity within the MFH treated cells as compared with the control samples. This is evidence for effective, spatially focused MFH therapy actuated and monitored during Lissajous scanning MPI.

IV. Conclusions

The presented study demonstrates the ability of MPI to act as a multi-functional platform to facilitate safe and optimised MFH therapy. The MPI scanner can be used to verify that the MNP heating agent is correctly located in the tumour before therapy, provide spatially focussed precision heating which can be used to further refine the volume which receives a heat dose, and for real-time thermal imaging of the heating as it occurs.

Acknowledgments

This project was supported by the DFG research grants "quantMPI: Establishment of quantitative Magnetic Particle Imaging (MPI) application oriented phantoms for preclinical investigations" (grant TR 408/9-1) and "Matrix in Vision" (SFB 1340/1 2018, no. 372486779, projects A02 and B02).

Author's statement

Conflict of interest: Authors state no conflict of interest.
Informed consent: Informed consent has been obtained from all individuals included in this study.

References

[1] X. Liu et al. Comprehensive understanding of magnetic hyperthermia for improving antitumour therapeutic efficacy, Theranostics (2020) 10(8): 3793-3815

[2] I. Rubia-Rodriguez et al., Whither magnetic hypertherthermia? A tentative roadmap, Materials (2021), 14(4), 706

[3] Z. W. Tay et al., Magnetic Particle Imaging-Guided Heating in Vivo Using Gradient Fields for Arbitrary Localization of Magnetic Hyperthermia Therapy, ACS Nano, 2018

[4] H. Paysen, J. Wells et al. Improved sensitivity and limit-of-detection using a receive-only coil in magnetic particle imaging. Phys. Med. Biol. (2018), 63, 13

[5] J. Wells et al. Challenges and recommendations for magnetic hyperthermia characterization measurements, Int. J. Hyperth. (2021) 38, 1

[6] J. Wells, et al. Lissajous scanning magnetic particle imaging as a multifunctional platform for magnetic hyperthermia therapy Nanoscale, 2020, 12, 18342-18355.

[7] C. Stehning et al. Simultaneous magnetic particle imaging and temperature mapping using multi-colour MPI Vol 2 No 2 (2016): Int J Mag Part Imag

